Molecular Biology of the Cell
Vol. 15, 2652–2663, June 2004

PtdIns-specific MPR Pathway Association of a Novel WD40 Repeat Protein, WIPI49[V]

Tim R. Jeffries,* Stephen K. Dove,† Robert H. Michell,† and Peter J. Parker*‡

*Protein Phosphorylation Laboratory, Cancer Research UK London Research Institute, Lincoln's Inn Fields Laboratories, London WC2A 3PX, United Kingdom; and †Department of Biochemistry, University of Birmingham, Birmingham B15 2TT, United Kingdom

Submitted October 15, 2003; Revised February 5, 2004; Accepted February 20, 2004
Monitoring Editor: Suzanne Pfeffer

WIPI49 is a member of a previously undescribed family of WD40-repeat proteins that we demonstrate binds 3-phosphorylated phosphoinositides. Immunofluorescent imaging indicates that WIPI49 is localized to both *trans*-Golgi and endosomal membranes, organelles between which it traffics in a microtubule-dependent manner. Live cell imaging establishes that WIPI49 traffics through the same set of endosomal membranes as that followed by the mannose-6-phosphate receptor (MPR), and consistent with this, WIPI49 is enriched in clathrin-coated vesicles. Ectopic expression of wild-type WIPI49 disrupts the proper functioning of this MPR pathway, whereas expression of a double point mutant (R221,222AWIPI49) unable to bind phosphoinositides does not disrupt this pathway. Finally, suppression of WIPI49 expression through RNAi, demonstrates that its presence is required for normal endosomal organization and distribution of the CI-MPR. We conclude that WIPI49 is a novel regulatory component of the endosomal and MPR pathway and that this role is dependent upon the PI-binding properties of its WD40 domain.

INTRODUCTION

Lysosomal biogenesis and homeostasis requires the sorting of nascent lysosomal enzymes away from secretory cargo at the *trans*-Golgi Network (TGN; Rohn *et al.*, 2000). The mannose-6-phosphate recognition system is a critical component of this trafficking pathway (Ghosh *et al.*, 2003). Posttranslationally, lysosomal enzymes acquire the mannose-6-phosphate marker and, subsequently, mannose-6-phosphate receptors (MPRs) coordinately bind to both this tag and components of clathrin-coated vesicles (CCVs) such as the coat adaptor protein-1 (AP-1) and also to GGA1 (Doray *et al.*, 2002). This capacity for dual interaction facilitates incorporation of lysosomal enzymes into endosome-bound transport vesicles budding from the TGN. On fusion of transport vesicles with endosomes the MPRs unload their bound ligands. Although soluble hydrolases released into the lumen of endosomes are ultimately delivered to lysosomes, the MPRs are retrieved from late endosomes back to the TGN for utilization in further rounds of sorting. This recycling to the Golgi requires the activity of both Rab9 and TIP47, a cytosolic protein recruited specifically to late endosomal membranes through its interactions with both Rab9 and MPRs (Carroll *et al.*, 2001).

A key component involved in endosomal operations is phosphatidylinositol 3-phosphate (PtdIns3P). PtdIns3P has been demonstrated to be involved in the processing of both the early and later stages of internalized cargo (Li *et al.*, 1995; Futter *et al.*, 2001). This effect is thought to be mediated through its interaction with defined protein modules such as the FYVE and PX domains (Misra *et al.*, 2001). EEA1 and Hrs are two endosomal proteins that both contain a FYVE domain (Simonsen *et al.*, 1998; Urbe *et al.*, 2000; Raiborg *et al.*, 2001). Although EEA1 is involved in mediation of early endosomal functions relating to homotypic endosome fusion as well as that of endocytosed vesicles with early endosomes (Rubino *et al.*, 2000; Lawe *et al.*, 2002), Hrs is involved in later events dealing with the sorting of cargo destined for degradation away from recycling proteins (Raiborg *et al.*, 2001; Raiborg *et al.*, 2002). A further FYVE domain–containing protein is the PtdIns3P 5-kinase, PIKfyve/p235 (McEwen *et al.*, 1999; Sbrissa *et al.*, 1999). PIKfyve has been localized to *trans*-elements of the Golgi as well as late endosomal compartments (Shisheva *et al.*, 2001). Whether the subcellular distribution of PIKfyve is dependent on the FYVE domain or whether the FYVE domain is solely utilized to facilitate processive phosphorylation is unclear (Sbrissa *et al.*, 2002a). PtdIns3,5P_2 plays a role in late endosomal dynamics in both yeast and mammalian cells. In yeast, *fab1* (fab1p is the yeast ortholog of PIKfyve) mutants display vacuolar acidification defects and a dramatic increase in vacuolar size (Gary *et al.*, 1998). This is at least partially due to a requirement for PtdIns3,5P_2 in inward vesiculation events in endosomal compartments (Odorizzi *et al.*, 1998). Although a direct role of PtdIns3,5P_2 within the operations of the mammalian endolysosomal system has not been shown directly, expression of a dominant-negative PIKfyve

Article published online ahead of print. Mol. Biol. Cell 10.1091/mbc.E03–10–0732. Article and publication date are available at www.molbiolcell.org/cgi/doi/10.1091/mbc.E03–10–0732.

[V] Online version of this article contains supporting material. Online version is available at www.molbiolcell.org.

‡ Corresponding author. E-mail address: Peter.Parker@Cancer.Org.Uk.

Abbreviations used: AP-1, adaptor protein complex 1; CCVs, clathrin-coated vesicles; CI-MPR, cation-independent MPR; MPR, mannose-6-phosphate receptor; MVB, multivesicular body; PtdIns, phosphatidylinositol; PI, phosphoinositide; TGN, *trans*-Golgi network; Vps, vacuolar protein sorting.

within Cos7 cells leads to endomembrane swelling and vacuolation (Ikonomov *et al.*, 2001). This effect can be rescued by injection of PtdIns3,5P_2 (Ikonomov *et al.*, 2001). Further support for a role of PI derivatives in multivesicular body (MVB) generation comes from microinjection studies using inhibitory antibodies directed against the PI3Kinase, hVPS34 (Futter *et al.*, 2001). Such treatment of Cos7 cells leads to an abrogation of internal vesicle formation as well as a gross swelling of endosomal compartments as assayed by EM. Whether this phenotype reflects a direct role of PtdIns3P in MVB generation or simply the failure to generate the substrate for PIKfyve is unclear. PIKfyve has also been implicated in insulin signaling (Shisheva *et al.*, 2001), a cellular event that includes recruitment of the GLUT4 glucose transporter from internal endosomal regions to the plasma membrane (Haruta *et al.*, 1995).

Although numerous PtdIns3P binding proteins have been identified, to date only the PX domain–containing protein Sorting Nexin 1 has been reported to possess PtdIns3,5P_2 binding potential (Cozier *et al.*, 2002). In this study we report the identification of a novel phospholipid binding protein, WIPI49. WIPI49 binds PtdIns3P and, to a lesser extent, PtdIns3,5P_2 and PtdIns5P. WIPI49 is localized in a phosphoinositide (PI)-dependent manner to both endosomal and Golgi membranes within cells, where it has the capacity to regulate the trafficking of proteins involved in the MPR recycling pathway.

MATERIALS AND METHODS

Antibodies and Reagents

Antibodies against WIPI49 were raised in rabbits using a peptide corresponding to its C-terminal 20 amino acids (NEFPPIILCRGNQKGKTKQS), which had been conjugated to keyhole limpet hemocyanin (Calbiochem, La Jolla, CA). Sera were immunopurified using standard procedures after the peptide had been conjugated to actigel resin (Sterogene Bioseparations, Arcadia, CA). Other antibodies used in this study were murine anti-GM130 (Transduction Laboratories, Lexington, KY), murine anti-p230 (Transduction Laboratories), murine antigamma adaptin (Transduction Laboratories), goat anti-EEA1 (Santa Cruz Biotechnology, Santa Cruz, CA), rabbit anti-CI MPR (Gift of Dr Sharon Tooze), monoclonal 9E10 antimyc and monoclonal 3E1 anti-GFP (Central Services, CRUK, London).

Cloning and Expression of WIPI49

A full-length ORF for WIPI49 was amplified from IMAGE clone 752767 by PCR using the 5′ primer WIPI49f, which contained a *Hin*dIII site, (GGAGGC**AAGCTT**CGATGGACGCTCCCCCGGGC) in combination with the 3′ primer WIPI49r, which contained an *Eco*RI restriction site, (GTGTGC**GAATTC**AGTCATGACTGCTTCGTTTTGCC) (bold text refers to incorporated restriction site throughout). The resultant PCR product was cloned into pCR-Script (Stratagene, La Jolla, CA). After sequencing to confirm fidelity of amplification, the WIPI49 ORF was spliced into pEGFP-C1 and pDsRED2-C1 vectors (CLONTECH, Palo Alto, CA) by restriction digest with *Eco*RI and *Hin*dIII. A Myc-tagged version of WIPI49 was constructed by amplification of WIPI49 by the 5′ primer MycWIPI49f, which contained an *Eco*RI site (CTC**GAATTC**GCGATGGACGCTCCCCCGGGCGGG) and the 3′ primer MycWIPI49r, which contained a *Hin*dIII site (GGT**AAGCTT**TGACTGCTTCGTTTTGCCCTTC), and the amplified product was cloned into pCR-Script, sequenced, and subsequently inserted into pcDNA3.1-Myc by restriction digest with *Eco*RI and *Hin*dIII. To express WIPI49 in mammalian cells as a GST fusion the WIPI49 ORF was amplified by PCR using the 5′ primer WIPIGSTf, which contained a *Pst*I site (TCGAGC**CTGCAG**TTATGGACGCTCCCCCGGGCG) in conjunction with the 3′ primer WIPIGSTr, which contained a *Not*I site (TGCAGA**GCGGCCGC**GACTGCTTCGTTTTGCCC). The PX domain of Snx3 was amplified using the primer combination gSnx3Pxf (GACGCCTAC**CTGCAG**ATGAGCAACTTCCTCGAGATCGACG) and gSnx3Pxr (CGGACCGT**GCGGCCGC**GCATGTCTTATTTTAGATGGAG).

Postamplification the PCR product was cloned into pCR-Script, sequenced to confirm fidelity and subsequently spliced into pMT2-SM-GST by restriction digest with the enzyme combination *Not*I and *Pst*I.

The WIPI49 R226A, R227A mutant was generated by megaprimer mutagenesis PCR. The megaprimer was generated by amplification of the first 680 bases of NP_060453 with the 5′ primer 49f (CGAGCTCAAGCTTCGATGGACGCTCCCCCGGGCG) and the 3′ primer 49RRr (CACATACCTTTTCATCGC**TGCAGC**GGCCTCATAGAGCTTTTGCCC, mutated bases shown in bold). The amplified product was gel-purified and used in a second round of PCR in combination with 49r (ACTGCAGAATTCTCATGACTGCTTCGTTTTGCC). The resulting product (49RR) was digested with *Hin*dIII and *Eco*RI before splicing into pEGFP or pDsRED2. For generation of the GST-fusion vectors, 49RR was amplified using the primer combination WIPIGSTf and WIPIGSTr (see above), and the product was inserted into pMT2-GST by restriction digest with *Not*I and *Pst*I.

Cell Culture and Transfection

African Green monkey (Cos7) cells were grown in DMEM supplemented with 10% FCS, 2 mM glutamine, 100 μg/ml penicillin, 100 μg/ml streptomycin at 37°C in a humidified atmosphere of 10% CO_2. Cells were transiently transfected with plasmids of interest using LIPOfectamine 2000 (Invitrogen, Carlsbad, CA) according to the manufacturer's instructions. Cells were typically analyzed 36 h posttransfection.

Bioinformatics

Sequences were aligned using ClustalX and alignments saved in GCG-MSF format before preparation for presentation in MacBoxShade. Phylogenetic trees were prepared by bootstrapping in ClustalX and presented using NJPlot. Identity/similarity matrices were generated using MacBoxShade (www.ISREC.ISB-S1B.CH/ftp-server/boxshade/macboxshade/). Structural predictions were determined using the 3D-PSSM at URL: www.sbg.bio.ic.ac.uk/3dpssm/.

Drug Treatments

For the inhibition of PtdIns3K cells were serum-starved for 1 h before treating with 10 μM LY294002 for the times indicated. To disrupt the microtubule cytoskeleton, cells were treated with 10 μg/ml nocodoazole for the times indicated.

Immunofluorescence

Cells seeded on glass coverslips were washed with PBS before fixing in 4% PFA for 10 min at room temperature. After fixation cells were rinsed with PBS, permeabilized for 5 min in 0.2% Triton X-100, rinsed with PBS, and blocked in 1% BSA for 30 min. Cells were subsequently incubated with primary antibody for 2 h, washed four times with PBS, incubated with the relevant secondary antibodies for 1 h, washed three times with PBS and once with water, and finally mounted in Mowiol. 4–88 (Calbiochem). Slides were examined using a confocal laser scanning microscope (Axioplan2 with LSM510; Carl Zeiss, Thornwood, NY) equipped with a 63×/1.4 plan-APOCHROMAT oil immersion objective.

Live Cell Time-Lapse Imaging

For live cell imaging cells were grown on 35-mm glass-bottom microwell dishes (Matec, Northborough, MA). Imaging was performed in an environmental chamber at 37°C supplemented with 5% CO_2. Cells were maintained in phenol red–free DMEM containing 10% FBS. Cells were examined 20–24 h posttransfection using an Olympus IX70 microscope fitted with a Wallac UltraVIEW Confocal Scanner (Perkin Elmer-Cetus, Boston, MA), an E-662 LYPZT Amplifier Pieza Disk using the UltraVIEW Imaging Suite software package in Temporal Module setting (Perkin Elmer-Cetus). DsRED2 chimeric proteins were excited at 565 nm and detected at an emission wavelength of 583 nm, whereas GFP chimeras were excited at 488 nm and detected with a split emission spectrum of 525/550 nm. Quicktime movies were constructed from sets of sequential TIFFs using the AQM 2001 Kinetic Acquisition Manager software (Kinetic Imaging Ltd., Liverpool, United Kingdom).

Purification of GST-fusion Proteins

GST-fusion proteins were expressed in Cos7 cells transfected with pMT2-SM constructs containing the ORF of interest. Cells were allowed to express the fusion protein for 36 h after transfection before harvest in lysis buffer (150 mM NaCl, 50 mM Tris-HCl, pH 7.4, 0.5% NP40). Lysates were clarified by centrifugation at 25,200 × *g* for 10 min at 4°C before addition to GSH-Sepharose beads (Amersham, Amersham, UK), which had been washed previously in lysis buffer. GST-fusion proteins were incubated with beads overnight at 4°C with tumbling on a rotary wheel. After binding, beads were washed five times with 10 volumes of lysis buffer, and GST-fusion protein was eluted with 10 mM reduced GSH, 50 mM Tris-HCl, pH 8.0.

Liposome-binding Assay

Liposomes were prepared according to a protocol based on that of Cozier *et al.* (2002). Briefly, lipid mixtures of brain-derived phosphatidylethanolamine (Avanti, Birmingham, AL), synthetic dioleyl-phosphatidylserine (Avanti) and synthetic 1-palmitoyl-2-oleyl-phosphatidylcholine (Avanti) supplemented with specific diC16 phosphoinositides (Cell Signaling Technology, Beverly, MA) were dried under a stream of nitrogen in glass tubes to form a film of lipid. A 10× lipid stock buffer (20 mM KCl, 20 mM HEPES, pH 7.4, 0.2 mM EDTA) was added to the dried lipids and liposomes generated in a bath sonicator adaptor of a Branson Sonifier 250 sonicator (Danbury, CT). Aggre-

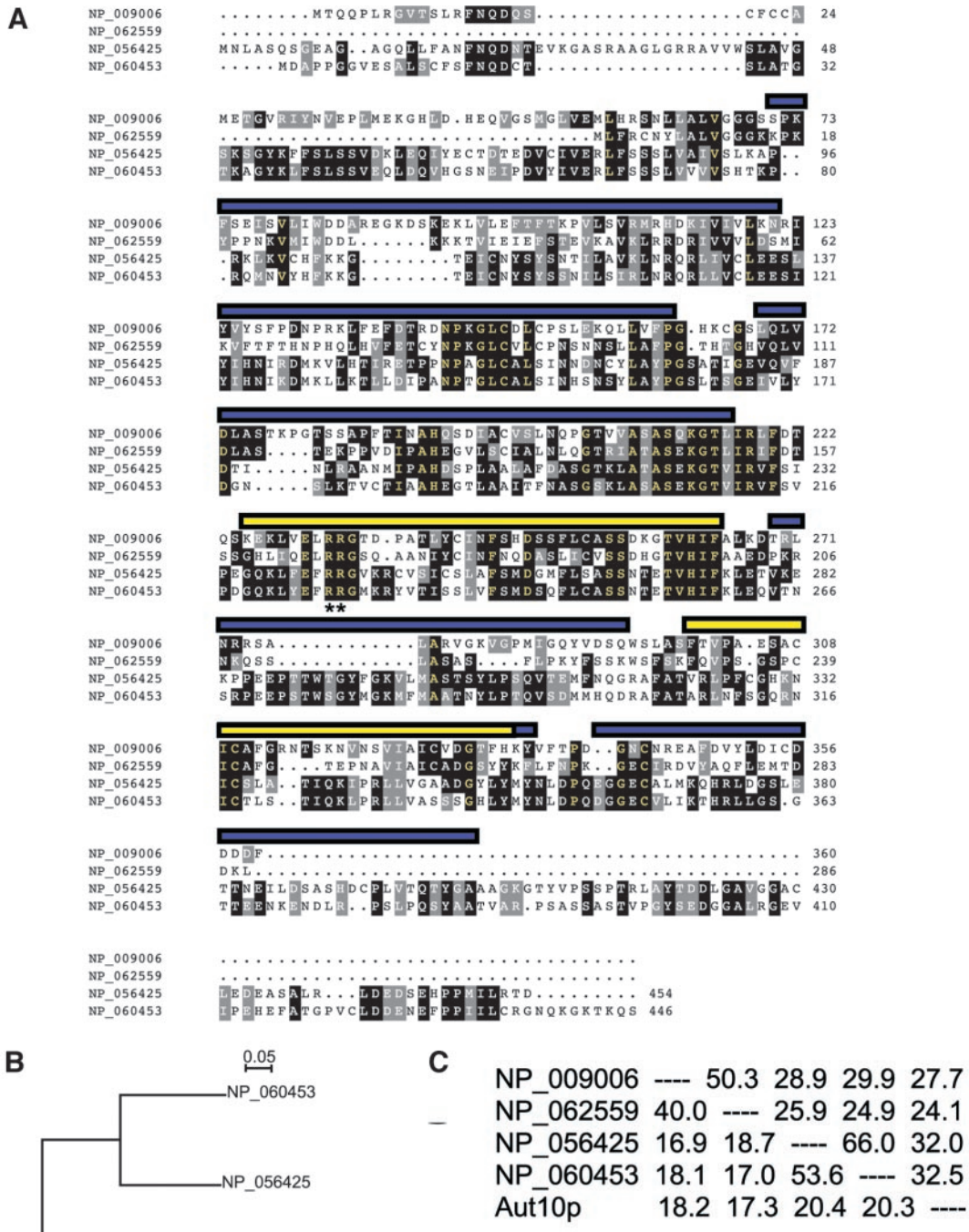

Figure 1. Identification of a novel family of mammalian WD-40 repeat containing proteins. (A), Sequence alignment of the four mammalian Aut10p homologues. Sequences were aligned using ClustalX and displayed using MacBoxShade. Normal residues are black text on white background, conserved residues are white text on black background, similar residues are white text on gray background, and identical residues are yellow text on black background. The predicted location of the seven WD40 motifs inferred by 3D modeling of the protein sequences are indicated by both the blue and yellow bars, whereas the location of WD40 repeats identified through primary sequence analyses are represented by yellow bars only. Double asterisks (**) indicate the position of a RR motif conserved throughout the protein family shown (B). Phylogenetic analysis of the evolutionary relationship between NP_009006, NP_062559, NP_056425, NP_060453, and Aut10p indicates that the human homologues of Aut10p comprise two separate lineages. (C). Similarity and identity matrix derived from protein sequences using MacBoxShade algorithms. Both the phylogenetic tree shown in B and the similarity/identity matrix presented in C indicate that all four human Aut10p homologues are approximately equally distant in terms of divergence from Aut10p.

gated material was removed by centrifugation of lipids in an Eppendorf centrifuge at 14,000 rpm for 10 min before dilution of liposomes into a 1× reaction buffer (0.12 M NaCl, 0.1 mM EGTA, 0.2 mM $CaCl_2$, 1.5 mM $MgCl_2$, 1 mM DTT, 5 mM KCl, 20 mM HEPES, pH 7.4, 1 mg/ml ovalbumin). Protein (250–500 ng) was incubated with liposomes for 10 min at room temperature before centrifugation at 100,000 × *g* for 30 min in a TL100 bench-top ultracentrifuge. Supernatants were removed and pelleted material resolved by SDS-PAGE.

Biosynthetic Labeling of Cathepsin D

Cathepsin D was labeled with [^{35}S]methionine (Amersham) essentially as previously described (Davidson, 1995). Briefly, transfected Cos7 cells grown on 35 × 10-mm Petri dishes were starved for 3 h in DMEM lacking methionine, supplemented with 10% FCS, which had been dialyzed, for 3 h. Cells were then labeled with 125 μCi [^{35}S]methionine for 30 min. Postlabeling cells were washed twice with DMEM/10%FCS and then chased for 3 h in normal media. Subsequent to chasing, cell media was collected and reserved, and cells were washed twice in PBS and lysed in lysis buffer (150 mM NaCl, 50 mM Tris-HCl, 0.5% NP40, mini-complete protease inhibitors; Sigma, St. Louis, MO) and clarified by centrifugation for 10 min. Then equivalent amounts of cellular media and cell lysates were precleared with protein A before immunoprecipitation with monoclonal anti-cathepsin D (Serotec, Oxford, UK) at 4°C overnight. Postprecipitation antibody-protein conjugates were harvested using protein A-Sepharose beads, and beads then were washed extensively in lysis buffer before resolution of immunoprecipiates by SDS-PAGE. After electrophoresis gels were stained with Coomassie, treated with ENHANCE (New England Nuclear, Boston, MA), dried down, and then exposed to a phosphoimager.

Isolation of Clathrin-coated Vesicles from Rat Brain

Ten rat brains were washed in buffer 1 (25 mM HEPES, pH 7.4; 125 mM potassium acetate; 5 mM magnesium acetate; 1 mM DTT), resuspended to a volume of 40 ml and homogenized with 20 strokes of a Potter homogenizer. Homogenates were spun at 8000 × *g* in an SS34 rotor for 20 min, and supernatant was collected and ultracentrifuged at 150,000 × *g* for 40 min in a 70Ti rotor. The pellet was resuspended in 10 ml of buffer 1, homogenized, and added to an equal volume of buffer 1 containing 12.5% Ficoll and 12.5% sucrose. The resultant solution was spun in a 70Ti rotor at 46,000 × *g* for 20 min, and the supernatant was diluted 1:5 in buffer 1 and ultracentrifuged at 95,000 × *g* for 60 min in a 45Ti rotor. The pellet was homogenized in 15 ml of buffer 1 and left on ice for 1 h after which it was spun at 16,000 × *g* for 10 min. Finally the supernatant was spun at 80,000 × *g* in an SW40 rotor for 2 h to pellet CCVs.

Preparation of Cos7 Cell Lysate Fractions

For examination of endosomal densities, Cos7 cells were scraped and washed in PBS before resuspension in homogenization buffer (HB; 0.25 M sucrose, 0.5 mM EDTA). Cells were burst by passing through a Cellcracker (HGM) and a postnuclear supernatant (PNS) prepared. The PNS was layered onto a continuous sucrose gradient ranging from 21% sucrose to 54% sucrose and centrifuged in a SW40 rotor at 87,000 × *g* overnight. After centrifugation 24 fractions were collected and each resolved by SDS-PAGE.

RNAi

RNAi was conducted using the pSUPERpuro system (OligoEngine, Seattle, WA). Three specific 23-base long regions were selected from the DNA sequence of WIPI49. These were incorporated into a synthetic 64mer oligonucleotide designed for hairpin RNA expression. Both sense and antisense oligonucleotides were made. The three pairs of oligonucleotide were annealed to each other and subsequently inserted into pSUPERpuro. The primer combinations used are as follows: for pSUPERpuro-WIPI49I, RNAiWIPI49f2 g a t c c c c g t t a t t c c t g a a c a t g a g t t t c a a g a g a a c t c a t g t t c a g g a a t a a c t t t t t g g a a a a and RNAiWIPI49r2 a g c t t t t c c a a a a a g t t a t t c c t g a a c a t g a g t t c t c t t g a a a c t c a t g t t c a g g a a t a a c g g g, for pSUPERpuro-WIPI49II, RNAiWIPI49r8 a g c t t t t c c a a a a a g g t a t g t g a c a a t c a g c t c t c t t g a a g a g c t g a t t g t c a c a t a c c g g g and RNAiWIPI49f8 g a t c c c c g g t a t g t g a c a a t c a g c t c t t c a a g a g a g a g c t g a t t g t c a c a t a c c t t t t t g g a a a, for pSUPERpuro-WIPI49III, RNAiWIPI49f13 g a t c c c c g c c t g a c t t c a g g g g a g a t t t c a a g a g a a t c t c c c t g a a g t c a g g c t t t t t g g a a a a and RNAiWIPI49r13 a g c t t t t c c a a a a a g c c t g a c t t c a g g g g a g a t t c t c t t g a a a t c t c c c c t g a a g t c a g g c g g g. After confirmation of the constructs Cos7 cells were transfected with the appropriate plasmid, and transformants were selected for in media containing 2.5 μg/ml puromycin.

RESULTS

WIPI49, a Novel PtdIns3P-binding Protein

A novel mammalian gene family encoding potential phospholipid-binding proteins was identified on the basis of homology to the yeast PtdIns3,5P_2-binding protein SVP1 (Dove *et al.*, 2004), a protein also identified as being involved in autophagy, Aut10p (Barth *et al.*, 2001). The mammalian gene family comprises four members (Entrez protein identifiers NP_056425, NP_060453, NP_062559, and NP_009006). Although examination of these primary sequences with Pfam indicates the presence of three putative WD40 repeats (Figure 1A), inspection of each protein using structural prediction programs intimates that they fold to form β-propellers (confidence limit at least 95%), structural domains typically composed of six or seven WD40 repeats (Fulop and Jones, 1999). There are no other obvious domains present when NP_056425, NP_060453, NP_062559, and NP_009006 are aligned (Figure 1A), although the four proteins appear to form two subgroups with NP_009006 clustering with NP_062559, whereas NP_056425 groups with NP_060453. This subgrouping is corroborated both by phylogenetic tree analysis (Figure 1B) and by determination of the percentage similarity and identity between the sequence of each protein (Figure 1C). The yeast homolog, Aut10p, is approximately equidistant from all four mammalian proteins in terms of phylogenetic tree construction (Figure 1B), percentage similarities, and percentage identities (Figure 1C).

BLAST analysis of the mammalian SVP1 family ORFs using the TIGR Gene Indices EST analysis tool demonstrates that these genes are ubiquitously expressed (our unpublished data). Northern analysis using a multiple tissue expression array and a probe designed against the nucleotide

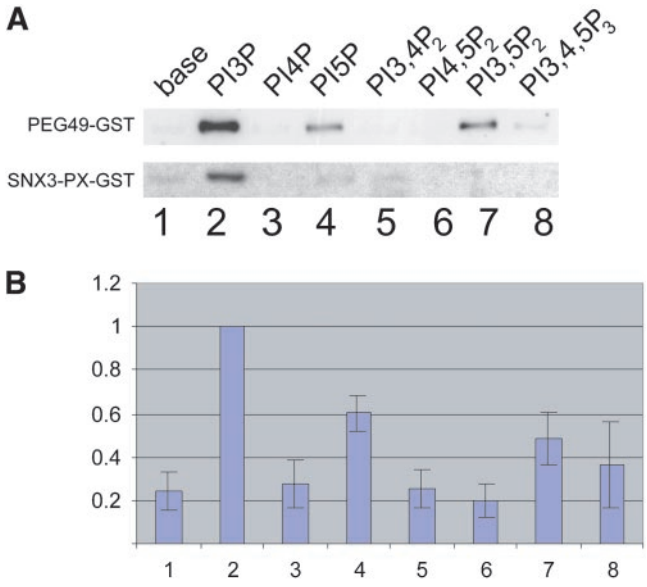

Figure 2. WIPI49 binds to PtdIns3P, PtdIns3,5P_2, and PtdIns5P in vitro. (A) Liposomes of defined phosphoinositide content were generated as described in MATERIALS AND METHODS and subsequently incubated with purified GST-WIPI49 or GST-SNX3-PX (~250 ng) for 10 min at 37°C. Resultant lipid complexes were pelleted by centrifugation, separated from supernatants, and resolved by SDS-PAGE and Western blotted using GST-specific antisera. Lane 1, base lipids; lane 2, PtdIns3P; lane 3, PtdIns4P; lane 4, PtdIns5P; lane 5, PtdIns3;4P_2; lane 6, PtdIns4,5P_2; 7, PtdIns3,5P_2; lane 8, PtdIns3,4,5P_3. (B) Data from seven independent liposome-binding experiments with GST-WIPI49 was quantified using NIH Image 1.6 and is presented using arbitrary binding values where material bound to PtdIns3P is equivalent to one unit. Error bars, SE. Lane 1, base lipids; lane 2, PtdIns3P; lane 3, PtdIns4P; lane 4, PtdIns5P; lane 5, PtdIns3,4P_2; lane 6, PtdIns4,5P_2; 7, PtdIns3,5P_2; lane 8, PtdIns3,4,5P_3.

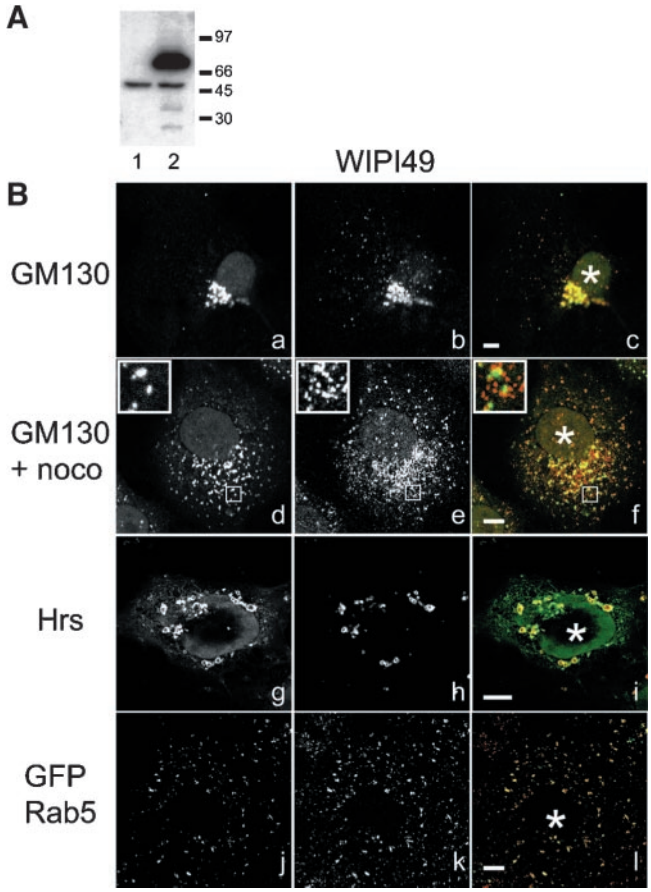

Figure 3. WIPI49 localizes to *trans*-Golgi and endosomal membranes. An antibody directed against the C-terminus of WIPI49 was raised in rabbits and affinity-purified. (A) Western blot analysis demonstrates anti-WIPI49 recognizes a single band of immunoreactivity 49 kDa in wild-type Cos7 lysates resolved by SDS-PAGE (lane 1). In COS7 cells transiently transfected with a plasmid encoding GFP-WIPI49, anti-WIPI49 detects both endogenous WIPI49 and a stronger second band of immunoreactivity at approximately 77 kDa that corresponds to GFP-WIPI49 (lane 2). (B) Cos7 cells were fixed in paraformaldehyde and processed for immunofluorescence using monoclonal anti-GM130 (a and d) and anti-WIPI49 (b and e). Merged images are shown in c and f. The cell shown in panels d, e, and f has been treated with nocodazole for 30 min before fixation to induce formation of Golgi ministacks. Cos7 cells transiently expressing Hrs-myc (g–i) were processed for immunofluorescence using murine anti-Myc (g and red in i) and rabbit anti-WIPI49 (h and green in i). The overexpression of Hrs results in WIPI49 accumulating in the Hrs-induced swollen endosomes. In addition, in Cos7 cells transfected with GFP-Rab5 (j–l) the Golgi localized pool of WIPI49 (k and red in l) is apparently redistributed to Rab5-positive endosomal regions. Asterisk (*) indicates position of the nucleus. Scale bar, 5 μm.

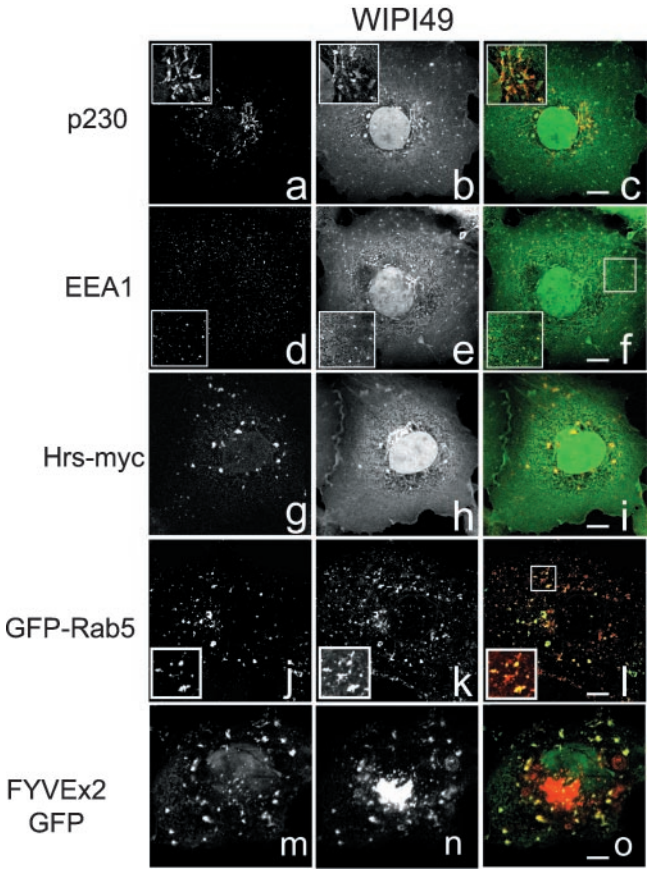

Figure 4. Transfected GFP- and DsRED2- tagged WIPI49 localize to the Golgi and endosomal membranes. Cos7 cells transiently expressing GFP-WIPI49 (a–c and d–f) were processed for immunofluroescence and stained with either murine anti-p230 to detect *trans*-Golgi elements (a and red in c) or goat anti-EEA1 to detect early endosomes (d and red in f). GFP-WIPI49 is observed to partially colocalize with p230 as well as a subpopulation of EEA1-positive membranes. To examine the relationship of WIPI49 to endosomes in more detail Cos7 cells were cotransfected with either Hrs-myc and GFP-WIPI49 (g–i) or with GFP-Rab5 and DsRED2-WIPI49 (j–l). Hrs-myc was detected by staining with murine anti-Myc (g and red in i) and observed to colocalize substantially with GFP-WIPI49 (h and green in i). In those cells expressing GFP-Rab5 (j and green in l) the DsRED2-WIPI49 (k and red in l) was seen to be localized predominately to Rab5-positive membranes with a significant reduction in the Golgi localized pool. To determine the relationship between the peripheral WIPI49 membranes and PtdIns3P-enriched regions Cos7 cells were cotransfected to express FYVEx2-GFP (m and green in o) in conjunction with DsRED2-WIPI49 (n and red in o). Although the perinuclear WIPI49 fluorescence is separated from the FYVEx2-GFP, there is some colocalization between the peripheral elements.

sequence of NP_060453 confirms this ubiquitous expression profile, although NP_060453 has the highest levels of mRNA in tissues of the heart and skeletal muscle (our unpublished results).

To begin characterization of this mammalian protein family, NP_060453 was cloned by PCR from the full-length IMAGE clone 752767.

To assess phosphoinositide binding potential, the association of purified NP_060453-GST to liposomes was investigated. As a positive control the PX domain of Snx3 (a domain previously identified as binding specifically to PtdIns3P) was expressed as a GST fusion (PX-Snx3-GST), and its phosphoinositide binding capabilities were tested in parallel. As expected, PX-Snx3-GST specifically bound to liposomes containing PtdIns3P (Figure 2). NP_060453-GST pelleted with liposomes that had incorporated a range of phosphoinositides (Figure 2). The highest levels of binding were observed with liposomes containing PtdIns3P, and, to a lesser extent, PtdIns5P and PtdIns3,5P_2.

Because of the phosphoinositide binding properties, as well as its predicted structure, NP_060453 is referred to as WD40 repeat protein Interacting with PhosphoInositides of 49kDa (WIPI49).

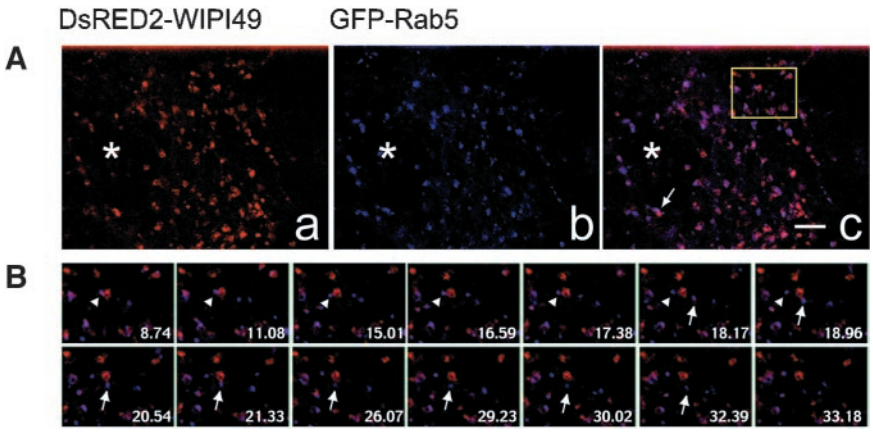

Figure 5. Dynamic relationship between DsRED2-WIPI49– and GFP-Rab5–positive membranes. See also Supplementary Video 4. Cos7 cells transfected with plasmids encoding DsRED2-WIPI49 (red) and GFP-Rab5 (blue) were analyzed by fluorescence microscopy. (A) DsRED2-WIPI49 (left), GFP-Rab5 (middle), and the merged image (right) in transfected cells. The arrow indicates a membrane compartment positive for both Rab9 and WIPI49 that undergoes coordinate movement and then segregation of the Rab9 and WIPI49 signals about two thirds of the way through the film. The boxed region in c relates to Figure 5B. (B) Enlarged selected video images from a time-lapse series corresponding to the boxed region from the cell represented in A. Overlay images show prolonged association of GFP-Rab5 with DsRED2-WIPI49 membranes before segregational movement of GFP-Rab5 away from the DsRED2-WIPI49 (arrowhead). Subsequent to this segregation, a second GFP-Rab5 structure transiently associates with the DsRED2-WIPI49 membrane and then trafficks away (arrow). *, nucleus. Bar, 3 μm. Frame time indicated relates to seconds.

WIPI49 Is Localized to the Golgi and Peripheral Endosomes

The specific binding of WIPI49 to PtdIns3P and to both PtdIns5P and PtdIns3,5P_2 suggested that this protein may localize to endosomal membranes. This possibility was explored by the generation of polyclonal antisera against the unique C-terminal 20 amino acids of WIPI49. Affinity-purified antibodies recognized a single immunoreactive band of approximately 49 kDa when used in Western blotting of whole Cos7 cell lysates (Figure 3A, lane 1). Furthermore, Western blot analysis of whole Cos7 cell lysates transfected with a GFP-WIPI49 fusion recognized a further band of 70 kDa, which corresponds to the predicted size of the GFP fusion protein (Figure 3A, lane 2). Both of these signals could be abrogated by prior addition of the immunizing peptide to the primary antiserum incubations (unpublished data). After establishing specificity of the anti-WIPI49 antibody with regards to Western blotting, the intracellular localization of endogenous WIPI49 was investigated (Figure 3B). Staining of Cos7 cells with anti-WIPI49 demonstrates two main foci of immunoreactive structures. The first resides in a perinuclear position and partially colocalizes with the Golgi resident protein GM130 (Figure 3B, a–c). Treatment of Cos7 cells with nocodazole to induce formation of Golgi ministacks indicates that this perinuclear WIPI49 immunofluorescence most likely represents *trans*-elements of the Golgi (Figure 3B, d–f). The second locus of anti-WIPI49 immunoreactivity comprises numerous punctate peripheral structures (Figure 3B, b). Although we were unable to satisfactorily identify these peripheral structures as representing endosomal compartments, when the subcellular localization of WIPI49 was investigated in Cos7 cells overexpressing Hrs, WIPI49 was observed to accumulate in the elaborated Hrs-positive endosomes (Figure 3B, g–i). Additionally, in Cos7 cells overexpressing GFP-Rab5 there is a depletion of the Golgi-localized WIPI49 and an accumulation in peripheral Rab5-positive endosomes (Figure 3B, j–l). Thus the dispersed punctate WIPI49 has the characteristics of representing an endosomal compartment.

Immunofluorescence analysis of Cos7 cells transiently expressing GFP-WIPI49 showed that the recombinant protein localized to subcellular structures very similar to those positive for endogenous WIPI49 (Figure 4). GFP-WIPI49 partially colocalizes with both the *trans*-Golgi marker p230 and EEA1 (Figure 4, a–c and d–f, respectively). This Golgi and peripheral membrane localization was also observed with recombinant DsRED2-WIPI49 (unpublished data). Coexpression of GFP-WIPI49 and Hrs-myc causes an accumulation of GFP-WIPI49 in Hrs-elaborated endosomes, whereas coexpression of GFP-Rab5 with DsRED2-WIPI49 saw an

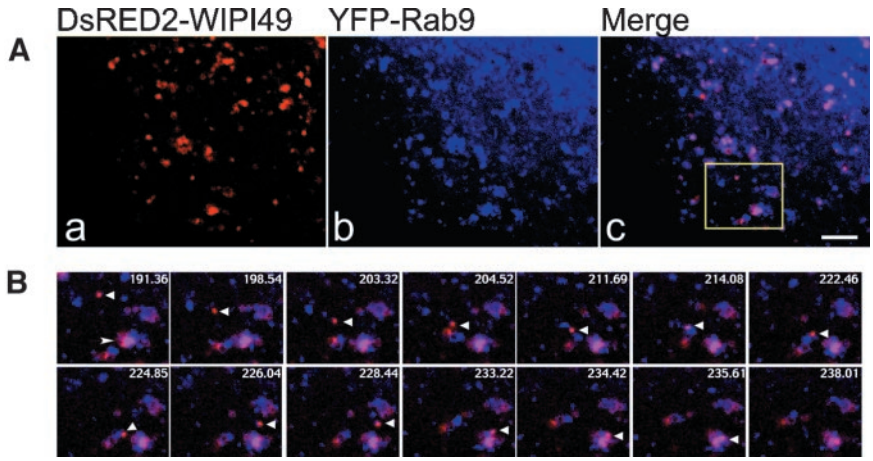

Figure 6. Migration of DsRED2-WIPI49 membranes to, and association with, Rab9-positive structures. See also Supplementary Video 5. Cos7 cells transfected with plasmids encoding DsRED2-WIPI49 (red) and YFP-Rab9 (blue) were analyzed by fluorescence microscopy. (A) DsRED2-WIPI49 (left), YFP-Rab9 (middle), and the merged image (right) in transfected cells. (B) Enlarged selected video images from a time-lapse series corresponding to the boxed region from the cell represented in A. Overlay images show directional trafficking of a DsRED2-WIPI49–positive vesicle (arrowhead) to, in addition to association and potential fusion with, a YFP-Rab9/DsRED2-WIPI49 endosome (arrow). Bar, 3 μm. Frame time indicated relates to seconds since commencement of filming.

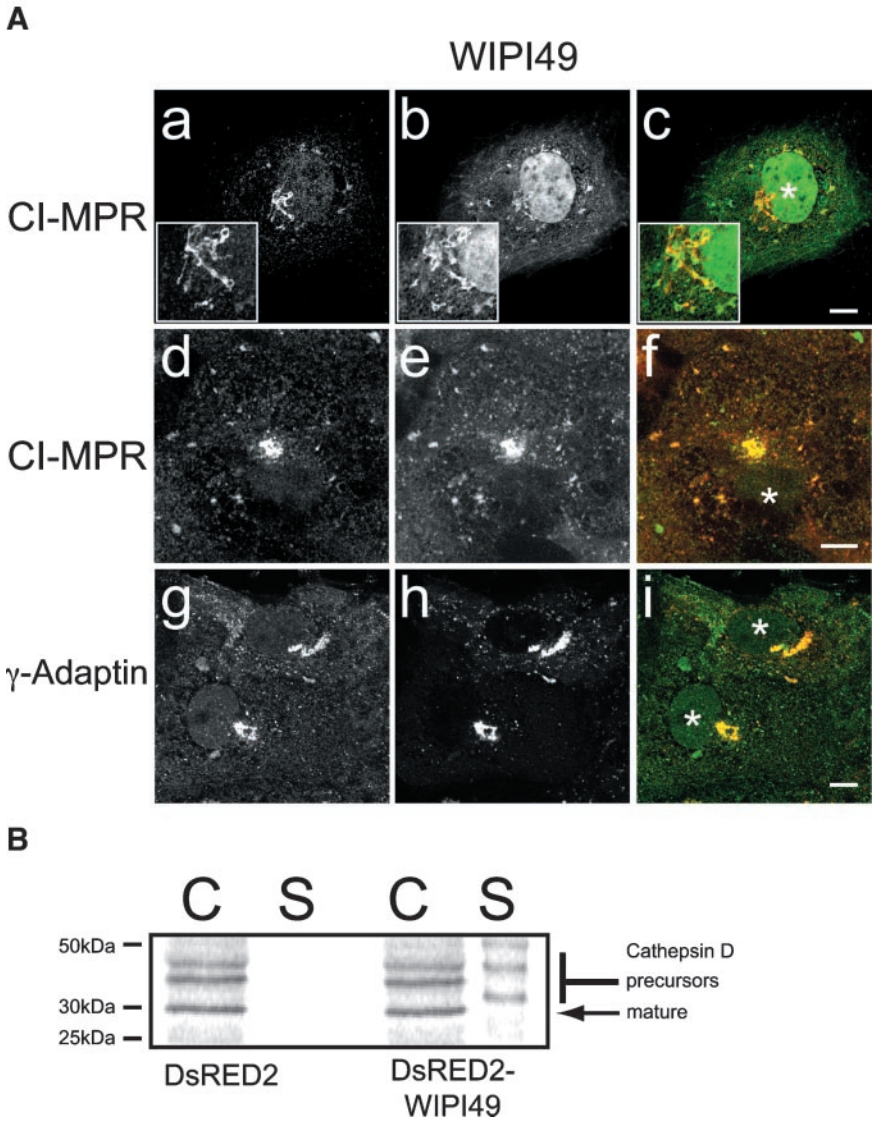

Figure 7. Perturbation of the mannose-6-phosphate pathway in Cos7 cells overexpressing WIPI49. (A) The subcellular distribution of the CI-MPR and γ-adaptin was examined in Cos7 cells transfected with either GFP-WIPI49 (a–c) or DsRED2-WIPI49 (d–f and g–i). In Cos7 cells transfected with GFP-WIPI49 (b and green in c) the CI-MPR (a and red in c) is observed to be localized in compartments positive for GFP-WIPI49. In Cos7 cells transiently expressing DsRED2-WIPI49 (e and red in f) there is again colocalization between the recombinant protein and CI-MPR, predominately in the perinuclear Golgi compartment. Examination of the γ-adaptin subunit of AP1 (g and green in i) in Cos7 cells expressing DsRED2-WIPI49 demonstrates substantial colocalization between the two proteins. (B) Overexpression of DsRED2-WIPI49 causes an increased secretion of cathepsin D precursor forms compared with cells transfected with DsRED2 only. Cos7 cells were transfected with either DsRED2 or DsRED2-WIPI49 were pulse-chased with ^{35}S-Met, and then cell-associated (C) and secreted (S) forms of cathepsin D were immunoprecipitated and resolved by SDS-PAGE before gel drying and exposure to a phosphoimager cassette.

attenuation in the perinuclear pool of DsRED2-WIPI49 and an apparent increase in the Rab5-positive endosomal pool (Figure 4, j–l). Furthermore, coexpression of, and subsequent colocalization between, DsRED2-WIPI49 with the PtdIns3P marker GFP-FYVEx2 further indicated that the peripheral WIPI49 membranes are endosomal in nature (Figure 4, m–o). The immunofluorescent examination of both endogenous WIPI49 and recombinant WIPI49 fusions indicates that WIPI49 is localized to both endosomal and *trans*-Golgi membranes, although there appears to be a higher ratio of peripheral material to perinuclear GFP-WIPI49 cells than to endogenous protein.

The epistatic relationship between WIPI49 and both Hrs and Rab5 suggested that WIPI49 may be cycling between the Golgi and endosomes, a possibility explored by live cell imaging of Cos7 cells transiently expressing GFP-WIPI49 or DsRED2-WIPI49. Live cell imaging of Cos7 cells transfected with GFP-tagged WIPI49 echoes the immunofluorescent data obtained from fixed cells in that WIPI49 is localized to both a perinuclear compartment (presumably the Golgi) and to peripheral structures (see Supplementary Videos 1 and 2). There is however a reduction in the number of cells with a discernable perinuclear focus of fluorescence, ~20% of transfectants have a clear perinuclear signal. The peripheral structures are motile and undergo both long- and short-range movements in a bidirectional manner (Supplementary Video 1).

Kinetic analyses of the WIPI49-positive structures indicate that they move with velocities very similar to those previously described for endosomal membranes (unpublished data and Gasman *et al.*, 2003) The movements of the WIPI49-positive compartments were investigated further by transiently coexpressing DsRED2-WIPI49 and a β-tubulin GFP chimera (GFP-Tub). The peripheral WIPI49 structures migrate along microtubules (Supplementary Video 3).

WIPI49 Is Involved in MPR Trafficking

The identity of the peripheral WIPI49 structures was investigated by comparison of the subcellular distribution and movement of ectopic WIPI49 against a range of endosomal Rab GFP constructs (specifically Rab 5, 7, 9 and 11). As noted above, cotransfection of Cos7 cells with both DsRED2-WIPI49 and GFP-Rab5 led to the ectopic WIPI49 being mainly concentrated within peripheral elements of the cell. Some of these structures were juxtaposed to and, partially

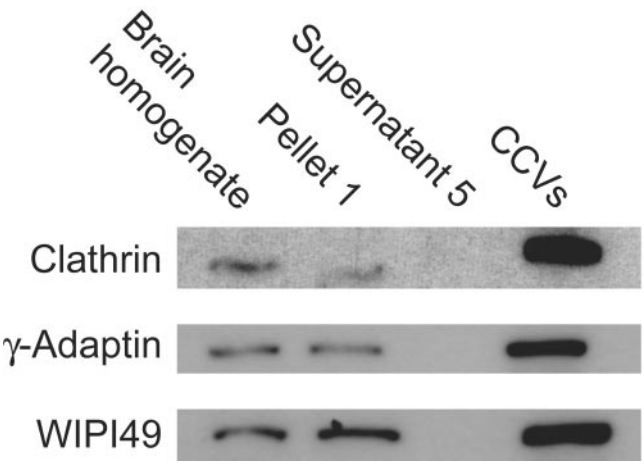

Figure 8. WIPI49 is enriched in clathrin-coated vesicles. An enriched CCV fraction was prepared from rat brain as described in the MATERIALS AND METHODS. After purification the relative amounts of clathrin, γ-adaptin, and WIPI49 were determined from equivalent levels of starting brain homogenate, and the initial pellet was retrieved after clarification of the homogenate and the enriched CCV fraction. Both clathrin and γ-adaptin are enriched in CCVs over the starting material, whereas WIPI49 has a lower degree of enrichment.

colocalized with, GFP-Rab5 (Figure 5 and Supplementary Video 4). Over time these structures moved coordinately with the GFP-Rab5 endosomal regions (see Supplementary Video 4) and some of the double-labeled endosomes underwent segregation events such that GFP-Rab5–enriched membranes migrated away from DsRED2-WIPI49 structures (Supplementary Video 4 and Figure 5B). Considering that Rab5-positive domains typically represent early endosomal structures involved in the initial processing of internalized material, we hypothesized that those peripheral DsRED2-WIPI49 structures not associated with GFP-Rab5 represent compartments involved in later cargo processing. To this end the relationship of DsRED2-WIPI49 with Rab7-positive lysosomes (Bucci *et al.,* 2000), Rab9-positive late endosomes (Lombardi *et al.,* 1993), and Rab11-positive recycling endosomes (Ullrich *et al.,* 1996) was investigated. There was a minimal relationship between DsRED2-WIPI49 structures with both GFP-Rab7 and GFP-Rab11 (aside from some juxtaposition with GFP-Rab7 structures; Supplementary Videos 5 and 6); in contrast, there was colocalization and juxtaposition between the ectopic WIPI49 and YFP-Rab9 (Figure 6 and Supplementary Video 7). These colocalizing and juxtaposed structures moved coordinately in both a Brownian manner and the stop-and-go manner characteristic of microtubule based movements. Notably, DsRED2-WIPI49 structures can be seen to traffic to and associate with YFP-Rab9 endosomes (Figure 6B).

The localization of WIPI49 to the Golgi, Rab5-endosomal regions and Rab9-positive structures suggested that this protein may operate within the MPR cycling pathway. Consequently the subcellular distribution of the CI-MPR was examined in the context of the ectopic expression of either GFP-WIPI49 or DsRED2-WIPI49 (Figure 7A). In Cos7 cells transiently expressing GFP-WIPI49, the CI-MPR partially colocalized with the ectopic protein, whereas in Cos7 cells expressing DsRED2-WIPI49 there was a greater colocalization between the CI-MPR and ectopic WIPI49. In cells expressing GFP-WIPI49 and those expressing DsRED2-WIPI49, there was an abberant localization of the CI-MPR. Rather than being distributed between the Golgi and endosomes, the MPR was found to reside predominately in perinuclear structures (Figure 7A, a–c and d–f).

Cells expressing DsRED2-WIPI49 had a more exacerbated phenotype in this respect than with GFP-WIPI49. The perturbation in the arrangement of CI-MPR immunoreactivity in Cos7 cells transfected with DsRED2-WIPI49 was examined further by comparison of the subcellular localization of the AP1 complex in DsRED2-WIPI49 transfectants (Figure 7A, g–i). The AP1 complex is involved in MPR trafficking and has been implicated in both anterograde and retrograde trafficking events between the *trans*-Golgi and endosomes (for review see Hinners and Tooze, 2003). In cells expressing DsRED2-WIPI49 it is clear that in a manner similar to that of CI-MPR, AP1 has a perturbed intracellular distribution such that it colocalizes with the perinuclear DsRED2-WIPI49 structure and lacks its wild-type distribution between the *trans*-Golgi network and endosomes (Figure 7A, g–i).

As immunofluorescence suggested there may be a defect in the MPR trafficking pathway in WIPI49 overexpressors, we examined the effect that overexpression of WIPI49 may have upon the delivery of cathepsin D to the lysosomes. Cathepsin D is a lysosomal hydrolase initially synthesized as a 53-kDa glycosylated precursor protein. After synthesis it is delivered to the lysosomes predominately via endosomes. Within lysosomes pro-cathepsin D undergoes deglycosylation and proteolysis to generate the mature form of the enzyme approximately 30 kDa in size. If the delivery of cathepsin D to the lysosomes is perturbed, for example in mice defective for AP1 functioning (Meyer *et al.,* 2000), then there is a concomitant increase in the secretion of precursor forms of cathepsin D into the cellular medium. Consistent with the hypothesis derived from immunofluorescent examinations of the subcellular localization of the CI-MPR in cells transiently expressing DsRED2-WIPI49 there was indeed an increase in the level of secreted precursor forms of cathepsin D into the cellular medium in those Cos7 cells transiently expressing DsRED2-tagged WIPI49 compared with those Cos7 cells transiently expressing DsRED2 alone (Figure 7B).

The relationship between WIPI49 and the MPR pathway was examined further by investigating whether WIPI49 is present in CCVs. Because WIPI49 seems to be traversing the MPR pathway in a manner that mimics the CI-MPR, then it should be packaged into CCVs. Comparison of the relative amount of WIPI49 between CCVs prepared from rat brain and whole brain homogenate shows that there is enrichment of endogenous WIPI49 with CCVs (Figure 8). This association with CCVs is consistent with all the evidence presented on the behavior of WIPI49, indicating that it traffics through the MPR pathway. The ability of WIPI49 to actively influence this traffic is evidenced by the disruption of MPR and AP-1 distribution on overexpression of WIPI49. To distinguish between a specific, compartment-associated effect of WIPI49 and a nonspecific effect, a mutant of WIPI49 was identified that had lost the ability to bind PIs (Figure 9A). This double arginine mutant (R226A, R227A) failed to interact with any of the three PIs identified for the wild-type protein. Expression of this mutant in Cos7 cells demonstrated that the loss of PI binding lead to a loss of membrane association and consequent to this the R226A, R227A WIPI49 mutant no longer influenced the distribution of MPR or γ-adaptin. Thus the specific compartment and traffic of WIPI49 requires the PI binding capacity of the protein, as does its influence on the behavior of this traffic. To corroborate the PI dependence of WIPI49 localization, the PI3Kinase inhibitor LY294002 was used to determine its effect on distribution. As shown in Figure 9C and Supple-

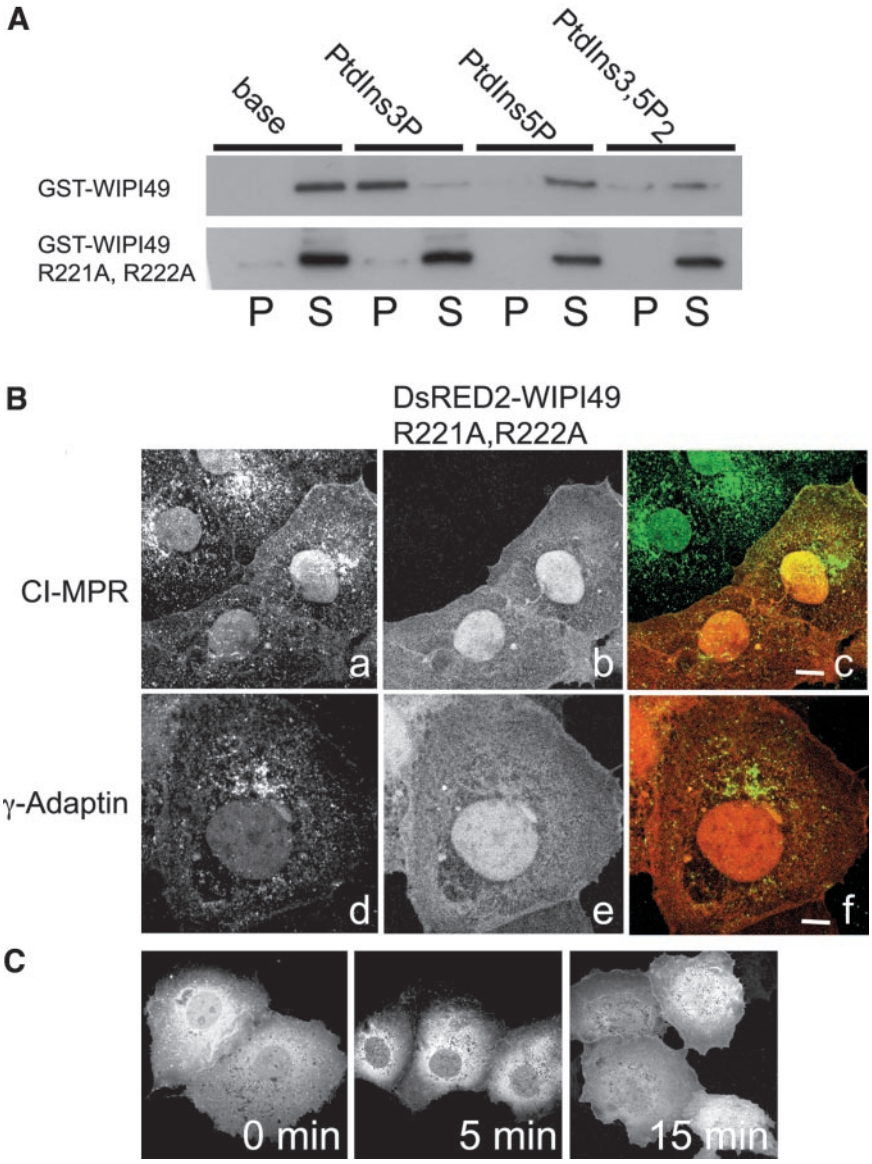

Figure 9. The PtdIns binding ability of WIPI49 is required for perturbation of the MPR pathway. (A) The ability of both GST-WIPI49 and GST-WIPI49 R226A, R227A to bind to base liposomes or liposomes that had incorporated PtdIns3P, PtdIns5P, or PtdIns3,5P_2 was compared. Material pelleting with liposomes (P) was resolved against the supernatant remaining after liposome pelleting (S). GST-WIPI49 binds to PtdIns3P containing liposomes (and to a lesser extent PtdIns5P/PtdIns3,5P_2 containing liposomes), whereas GST-WIPI49 R226A, R227A does not. (B) Ectopic expression of WIPI49 R226A, R227A does not disrupt the MPR pathway. When Cos7 cells are transfected with DsRED2-WIPI49 R226A, R227A (b and e and red in c, f) both the CI-MPR (a and green in c) and γ-Adaptin (d and green in f) have a normal subcellular distribution. Thirty-six hours posttransfection cells were fixed and stained with either rabbit anti-CI-MPR or mouse anti–γ-adaptin. (C) The requirement of WIPI49 interacting with PtdIns3P for its recruitment to membranes is supported by inhibition of PtdIns3P generation by the 3-kinase inhibitor LY294002. Cos7 cells expressing GFP-WIPI49 were treated with LY294002 for either 0, 5, or 15 min. After treating, cells were fixed and observed by immunofluroescence. Over time there is a loss of membrane-associated WIPI49.

mentary Video 8, acute treatment lead to a rapid loss of WIPI49 membrane localization.

To further investigate the role played by WIPI49 in endosomal dynamics RNA interference was used to knock down expression of the protein in Cos7 cells. Cells were transfected with either empty pSUPERpuro or pSUPERpuro constructs containing specific 64mer oligos designed to effect silencing of WIPI49 (pSUPERpuro-WIPI49I, II and III; see MATERIALS AND METHODS for details). After transfection and selection in puromycin for 2 weeks cell lysates were prepared and the degree of knockdown in WIPI49 levels was assessed by Western blotting. Figure 10A demonstrates that although both empty pSUPERpuro and pSUPERpuro-WIPI49I did not apparently affect protein levels of WIPI49, pSUPERpuro-WIPI49 II and III reduced the levels of protein by ~80%. Examination of WIPI49 knock-down cells by immunofluorescence suggested that the early endosomes were more elaborated than in wild-type cells, although the Golgi appeared normal (Figure 10B). The aberration in early endosomal architecture was confirmed by comparing the relative densities of early endosomes in knock-down cells with those isolated from wild-type cells by use of continuous sucrose density gradients. Figure 10C shows that in WIPI49 knock-down cells there is a shift of early endosomes to heavier fractions when compared with early endosomes isolated from wild-type cells. Finally, we examined whether WIPI49 knock-down cells also displayed alterations in the distribution of the CI-MPR across sucrose gradients. The CI-MPR is present across several fractions (presumably representing Golgi and late endosomal membranes in addition to early endosomal ones), and there is a shift of the CI-MPR to heavier fractions in the knockdown cells when compared with wild-type cells (Figure 10C).

DISCUSSION

The present study has described a novel phospholipid binding protein, WIPI49. WIPI49 is the defining member of a family of at least four mammalian genes, all of which share the same predicted seven-bladed beta propeller structure. Although the yeast homolog, Aut10p/Svp1p, groups weakly with NP_062559 and NP_009006 by phylogenetic

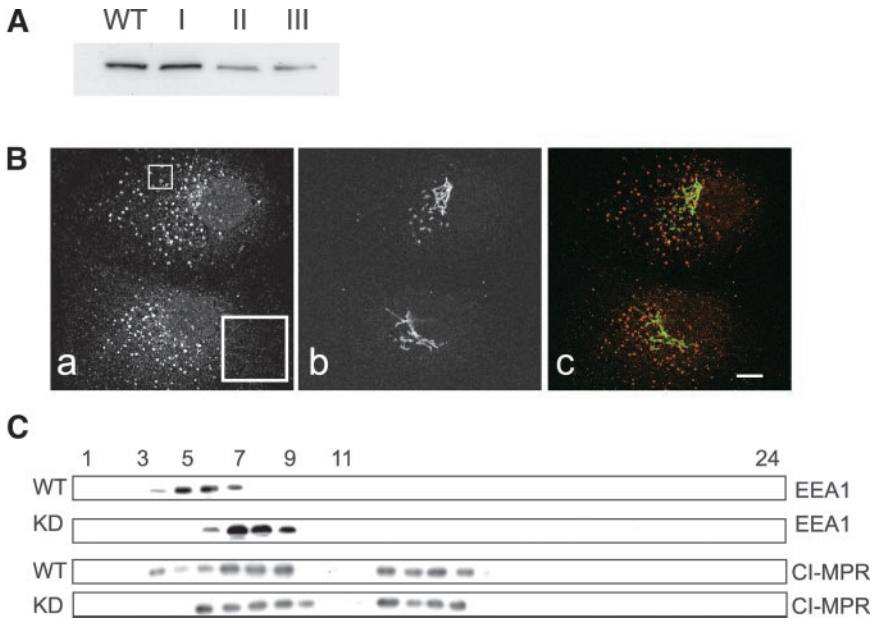

Figure 10. Suppression of WIPI49 expression by RNAi. (A) Cos7 cells transfected with either pSUPERpuro, pSUPERpuro-WIPI49I, pSUPERpuro-WIPI49II, or pSUPERpuro-WIPI49III were grown in media supplemented with 10 μg/ml of puromycin for 3 weeks before harvesting in sample buffer and resolution by SDS-PAGE. Subsequent to transfer to PVDF, the samples were probed with rabbit anti-WIPI49. It is clear that although neither pSUPERpuro nor pSUPERpuro-WIPI49I caused a reduction in the protein levels of WIPI49, both pSUPERpuro-WIPI49II and pSUPERpuro-WIPI49III do. (B) Cos7 cells transfected with pSUPERpuro-WIPI49II and selected for 3 weeks in puromycin were fixed in paraformaldehyde and processed for immunofluorescence using goat anti-EEA1 (a and red in c) and murine anti-GM130 (b and green in c). Although the morphology of the Golgi is normal, the early endosomes are more elaborate and larger than usual. The inset in "a" highlights the endosomal morphology. Scale bar, 5 μm. (C) Wild-type Cos7 cells (WT) or Cos7 cells with knocked down levels of WIPI49 (KD) were lysed and fractionated across a continuous sucrose gradient extending from 21 to 54% sucrose as described in MATERIALS AND METHODS. Subsequent to fractionation 24 fractions were collected (where fraction 1 is 21% sucrose and fraction 24 54% sucrose) and analyzed by Western blotting for the presence of EEA1 or CI-MPR.

analysis, comparison of percentage similarities and identities suggests it is more homologous in terms of sequence to NP_056425 and WIPI49. By these sequence analyses we conclude that Aut10p/Svp1p is equally distant, in evolutionary terms, from all four mammalian proteins. Because both WIPI49 and the yeast homolog (Dove *et al.*, 2004) can bind phosphoinositides, we consider it likely that all the WIPIs will have this capacity (see below) and that this mammalian gene family therefore constitutes a new class of phospholipid-binding proteins, which we refer to as the WIPIs.

A number of lines of evidence indicate that WIPI49 is a component of the Golgi–early endosome–late endosome–Golgi cycling pathway that is followed by receptor proteins involved in the delivery of lysosomal resident proteins (Ghosh *et al.*, 2003). Endogenous WIPI49 is localized to *trans* elements of the Golgi, endosomal membranes and is enriched in CCVs. The disruption in the localization of endogenous WIPI49 seen when either Hrs or Rab5 is overexpressed supports the notion that WIPI49 is dynamically cycling through these compartments and is therefore susceptible to conditions that modulate membrane flux through these compartments. This dynamic nature is further highlighted by videomicroscopy of Cos7 cells expressing fluorescent WIPI49 chimeras. WIPI49-positive membranes move in a microtubule-dependent manner with kinetics similar to those previously described for endosomes in HeLa cells (Gasman *et* al., 2003). The WIPI49 chimeric proteins are found on at least two distinct sets of endosomal membranes. Ectopically expressed WIPI49 partially colocalizes and moves coordinately with both Rab5-positive and Rab9-positive endosomes in live cells. Importantly, WIPI49 can be seen to segregate away from Rab5-positive structures as well as trafficking to and associating with Rab9-positive membranes.

Role of Phospholipids in the Endolysosomal Pathway

The binding of WIPI49 to liposomes incorporating PtdIns3P (or other 3-phosphorylated PIs) can be inhibited by mutation of arginine residues R221 and R222. This mutant fails to localize to membranes, a property also observed for wtWIPI49 when PtdIns3K activity is inhibited. These phenotypes lead us to conclude that WIPI49 is a novel PtdIns3P binding module. The complete conservation of the two critical arginine residues in the WIPI family is indicative of a conservation of PI-binding function for the entire WIPI family. The demonstration that the yeast ortholog Svp1 also binds a 3-phosphorylated PI (PtdIns3,5P_2) is entirely consistent with this conclusion. Alongside the FYVE domain, the PX domain and the KKPAKK motif of Etf1p (Wurmser and Emr, 2002), the identification of WIPI49 brings the total number of PtdIns3P binding modules identified to four. Although these motifs all allow interaction with PtdIns3P and a general localization to endosomal membranes, this lipid interaction alone is insufficient for a protein's precise subcellular address. For example, Hrs, EEA1, and PIKfyve all possess a FYVE finger motif, yet Hrs and EEA1 are localized to nonoverlapping early endosomal membranes, whereas PIKfyve has been localized to late endosomes (Shisheva *et al.*, 2001). Clearly other factors must be involved in the further compartmentalization of these proteins. The intracellular localization of WIPI49 is dependent on its ability to bind PIs. The fact that it can bind to PtdIns3P, PtdIns5P, and PtdIns3,5P_2 in vitro raises the question of which of these PI interactions are relevant in vivo. The metabolic interrelationship of these lipids makes it impossible currently to distinguish which lipid interaction dominates; however, the capacity to bind this range of interconverted PI species may explain the sequential localization of WIPI49 across at least three discrete types of membranes. This behavior would be consistent with the notion of sequential PI-dependent sorting functions.

Mutations inhibiting the lipid kinase activity of the PtdIns3P-5-Kinase Fab1, and consequently a lack of PtdIns3,5P_2, have previously been shown to result in multiple defects with regards to vacuolar function in budding yeast (Gary *et al.*, 1998). These include a failure of normal MVB formation due to a lack of inward budding events, a failure in acidification of the vacuole, and the formation of a grossly swollen vacuole, which occupies nearly the entire yeast cell body (Gary *et al.*, 1998). Studies in mammalian cells have also demonstrated a role for PtdIns3P in the proper functioning of the endolysosomal system. For example, inhibition of hVPS34 function results in a swelling of late endosomal elements. This effect cannot be solely explained in terms of a failure in MVB generation (i.e., budding of vesicles into the endosomal lumen) and probably results from a failure of membrane recycling from late endosomes back to donor compartments (Futter *et al.*, 2001). Whether these studies reflect a direct role of PtdIns3P in the functioning of the endolysosomal system or simply the requirement of PtdIns3P as a substrate for PIKfyve (the mammalian homolog of Fab1) is unclear. It is apparent though that there is a requirement for both PtdIns3P and PtdIns3,5P_2 in membrane recycling events occurring on late endosomes. In terms of a role for phospholipids in membrane dynamics, it is notable that WIPI49 has the capacity to bind to PtdIns3P as well as to PtdIns3,5P_2 and hence represents a protein with the capacity to link PtdIns3,5P_2 production to the proper functioning of late endosomes (Katzmann *et al.*, 2002). The delivery of membrane-associated WIPI49 away from Rab5-positive membranes toward Rab9-positive late endosomes will result in its localization to a region of the cell where PtdIns3P5Kinase activity resides (Shisheva *et al.*, 2001). WIPI49 may then bind to locally produced PtdIns3,5P_2 and function in one of the PtdIns3,5P_2 pathways in which this phospholipid has been implicated. Considering the relationship between WIPI49, MPR, and AP1 that has been described here, this PtdIns3,5P_2-dependent function would most likely represent a role in the trafficking of MPR into and/or out of endosomal membranes.

The hypothesis that WIPI49 cycles through the MPR pathway raises the question of how WIPI49 associates with membranes at the *trans*-Golgi and is enriched in CCVs. In this context it is interesting that EpsinR shares a subcellular distribution similar to that of WIPI49. Although EpsinR binds directly to clathrin and the AP1 complex (Hirst *et al.*, 2003; Mills *et al.*, 2003), we have been unable to detect any interaction between WIPI49 and the subunits of the AP1 complex (our unpublished observations), EpsinR, however, has also been shown to bind to PtdIns4P and PtdIns5P in vitro. PI4Kinase has been localized to the Golgi, and this enzymic activity has been suggested to be responsible for the Golgi localization of EpsinR (Mills *et al.*, 2003). However, the fact that both EpsinR and WIPI49 can bind PtdIns5P may be relevant with regards to Golgi localization. PtdIns5P has recently been recognized as a bona fide cellular phospholipid (Schaletsky *et al.*, 2003), although its means of synthesis is controversial. Some investigators believe that PIKfyve displays PI5Kinase activity on phosphatidylinositol to generate PtdIns5P (Sbrissa *et al.*, 2002b). However, in view of the lack of PtdIns5P in yeast overexpressing PIKfyve, it is perhaps more likely that PtdIns5P is derived from the action of the 3-phosphatase myotubularin (or a related 3-phosphatase) on PtdIns3,5P_2 (Schaletzky *et al.*, 2003). Both the region of synthesis and site of action of PtdIns5P is unknown; however, the relationship between EpsinR and WIPI49 may reflect a role for PtdIns5P at the *trans*-Golgi.

In addition to WIPI49 traversing the MPR pathway, mutagenic and ectopic expression studies point to WIPI49 acting as a regulatory component of this pathway. Although ectopic WIPI49 localizes to endosomal elements, there is a large amount of perinuclear DsRED2-WIPI49 associated with *trans*-elements of the Golgi. Although this pattern of localization is similar to that of endogenous WIPI49, within these Golgi-associated structures there is an aberrant accumulation of the CI-MPR and of AP1, an adaptor complex involved in traffic between the TGN and early endosomes. These observations, along with the increased secretion of precursor forms of cathepsin D in cells overexpressing WIPI49, lead us to conclude that it plays a regulatory role in the MPR pathway. The potential for WIPI49 to have a functional input to MPR trafficking is supported by the loss of the MPR pathway defect when a WIPI49 isoform incapable of binding PIs is expressed. Thus the presence of the protein per se is insufficient to disrupt this pathway, rather WIPI49 must retain its specific localization through PI interaction to exert this effect. Furthermore, this is not simply a reflection of PI interaction itself, because distinct patterns of traffic behvavior are observed when other PI-binding proteins are overexpressed, and in the context of Cos7 cells expressing ectopic WIPI49 there is a proper localization of coexpressed FYVEx2-GFP. It is unclear whether this defect in trafficking occurs in movements from the *trans*-Golgi to Rab5-positive membranes or from Rab9-positive late endosomes to *trans*-Golgi membranes. The mislocalization of the γ-adaptin subunit of AP1 in WIPI49 overexpressing cells suggests that the defect in lysosomal enzyme delivery represents a failure of traffic exiting the *trans*-Golgi. This defect is not a generalized nonspecific inhibition of all trafficking events from the Golgi because the secretory pathway is intact (our unpublished observations). To further discern the role of WIPI49, RNAi was used to knock down the WIPI49 protein levels. Although cells that have had protein levels knocked down by ~80% still process cathepsin D, normally (our unpublished data) there is an aberration in the structure of early endosomes such that they have an apparently enlarged size and appear more elaborate (Figure 10B). This elaboration of the early endosomes indicates a retardation in a pathway either at the level of material exiting the early endosomal regions to traffic to downstream compartments (e.g., late endosomes and recycling endosomes) or an increase in traffic into the endosomes. This depletion of WIPI49 levels causing an enlargement of endosomal structures is consistent with our hypothesis of WIPI49 acting as a PtdIns-sensitive regulatory component of the MPR pathway. The apparently normal processing of cathepsin D in WIPI49 knock-down cells is likely due to the fact that the residual levels of WIPI49 (~20% of normal) can fulfill this role in terms of cathepsin D traffic.

In summary, we have described a novel WD-40 repeat protein, WIPI49, that likely folds to form a β-propeller. WIPI49 binds to PtdIns3P, PtdIns5P, and PtdIns3,5P_2 and is localized to *trans* elements of the Golgi and throughout membranes of the endolysosomal network positive for Rab5 and Rab9. WIPI49 is a novel component of the MPR pathway and provides a previously undescribed means of coupling regulation of this pathway to PIs.

ACKNOWLEDGMENTS

We thank Susanne Pfeffer, Wanjin Hong, Harald Stenmark, George Banting, Miguel Seabra, William Buoy, and Bruno Goud for kind gifts of plasmids; Mike Mitchell for help with bioinformatics analysis; Gipi Schiavo for assistance with liposome binding assays; and Sharon Tooze, Richard Grose and

Michael Way for critical reading. This work was supported by Cancer Research UK.

REFERENCES

Barth, H., Meiling-Wesse, K., Epple, U.D., and Thumm, M. (2001). Autophagy and the cytoplasm to vacuole targeting pathway both require Aut10p. FEBS Lett. *508,* 23–28.

Bucci, C., Thomsen, P., Nicoziani, P., McCarthy, J., and van Deurs, B. (2000). Rab 7, a key to lysosome biogenesis. Mol. Biol. Cell *11,* 467–480.

Carroll, K.S., Hanna, J., Simon, I., Krise, J., Barbero, P., and Pfeffer, S.R. (2001). Role of Rab9 GTPase in facilitating receptor recruitment by TIP47. Science *292,* 1373–1376.

Cozier, G.E., Carlton, J., McGregor, A.H., Gleeson, P.A., Teasdale, R.D., Mellor, H., and Cullen, P.J. (2002). The phox homology (PX) domain-dependent, 3-phosphoinositide-mediated association of sorting nexin-1 with an early sorting endosomal compartment is required for its ability to regulate epidermal growth factor receptor degradation. J. Biol. Chem. *277,* 48730–48736.

Davidson, H.W. (1998) Worthannin causes mistargeting of procathepsin D: evidence for the involvement of a P13K in vesicular transport to lysomes, J. Cell Biol., *130,* 797–805.

Doray, B., Ghosh, P., Griffith, J., Geuze, H.J., and Kornfeld, S. (2002). Cooperation of GGAs and AP-1 in packaging MPRs at the trans-Golgi network. Science *297,* 1700–1703.

Dove, S.K., *et al.* (2004). Svp1p defines a family of phosphatidylinositol 3,5-bisphosphate effectors. Embo J. (*in press*).

Fulop, V., and Jones, D.T. (1999). Beta propellers: structural rigidity and functional diversity. Curr. Opin. Struct. Biol. *9,* 715–721.

Futter, C.E., Collinson, L.M., Backer, J.M., and Hopkins, C.R. (2001). Human VPS34 is required for internal vesicle formation within multivesicular endosomes. J. Cell Biol. *155,* 1251–1264.

Gary, J.D., Wurmser, A.E., Bonangelino, C.J., Weisman, L.S., and Emr, S.D. (1998). Fab1p is essential for PtdIns(3)P 5-kinase activity and the maintenance of vacuolar size and membrane homeostasis. J. Cell Biol. *143,* 65–79.

Gasman, S., Kalaidzidis, Y., and Zerial, M. (2003). RhoD regulates endosome dynamics through Diaphanous-related Formin and Src tyrosine kinase. Nat. Cell Biol. *5,* 195–204.

Ghosh, P., Dahms, N., M. and Kornfeld, S. (2003) Mannose 6-phosphate receptors: new twists in the tale. Nat. Rev. Mol. Cell. Biol. *4,* 202–212.

Haruta, T., Morris, A.J., Rose, D.W., Nelson, J.G., Mueckler, M., and Olefsky, J.M. (1995). Insulin-stimulated GLUT4 translocation is mediated by a divergent intracellular signaling pathway. J. Biol. Chem. *270,* 27991–27994.

Hinners, I., and Tooze, S.A. (2003). Changing directions: clathrin-mediated transport between the Golgi and endosomes. J. Cell Sci. *116,* 763–771.

Hirst, J., Motley, A., Harasaki, K., Peak Chew, S.Y., and Robinson, M. S. (2003). EpsinR: an ENTH domain-containing protein that interacts with AP-1. Mol. Biol. Cell *14,* 625–641.

Ikonomov, O.C., Sbrissa, D., and Shisheva, A. (2001). Mammalian cell morphology and endocytic membrane homeostasis require enzymatically active phosphoinositide 5-kinase PIKfyve. J. Biol. Chem. *276,* 26141–26147.

Katzmann, D.J., Odorizzi, G., and Emr, S.D. (2002). Receptor downregulation and multivesicular-body sorting. Nat. Rev. Mol. Cell. Biol. *3,* 893–905.

Lawe, D.C. *et al.* (2002). Sequential roles for phosphatidylinositol 3-phosphate and Rab5 in tethering and fusion of early endosomes via their interaction with EEA1. J. Biol. Chem. *277,* 8611–8617.

Li, G., D'Souza-Schorey, C., Barbieri, M.A., Roberts, R.L., Klippel, A., Williams, L.T., and Stahl, P.D. (1995). Evidence for phosphatidylinositol 3-kinase as a regulator of endocytosis via activation of Rab5. Proc. Natl. Acad. Sci. USA *92,* 10207–10211.

Lombardi, D., Soldati, T., Riederer, M.A., Goda, Y., Zerial, M., and Pfeffer, S.R. (1993). Rab9 functions in transport between late endosomes and the trans Golgi network. EMBO J. *12,* 677–682.

McEwen, R.K., Dove, S.K., Cooke, F.T., Painter, G.F., Holmes, A.B., Shisheva, A., Ohya, Y., Parker, P.J., and Michell, R.H. (1999). Complementation analysis in PtdInsP kinase-deficient yeast mutants demonstrates that Schizosaccharomyces pombe and murine Fab1p homologues are phosphatidylinositol 3-phosphate 5-kinases. J. Biol. Chem. *274,* 33905–33912.

Meyer, C., Zizioli, D., Lausmann, S., Eskelinen, E.L., Hamann, J., Saftig, P., von Figura, K., and Schu, P. (2000). mu1A-adaptin-deficient mice: lethality, loss of AP-1 binding and rerouting of mannose 6-phosphate receptors. EMBO J. *19,* 2193–2203.

Mills, I.G., Praefcke, G.J., Vallis, Y., Peter, B.J., Olesen, L.E., Gallop, J.L., Butler, P.J., Evans, P.R., and McMahon, H.T. (2003). EpsinR: an AP1/clathrin interacting protein involved in vesicle trafficking. J. Cell Biol. *160,* 213–222.

Misra, S., Miller, G.J., and Hurley, J.H. (2001). Recognizing phosphatidylinositol 3-phosphate. Cell *107,* 559–562.

Odorizzi, G., Babst, M., and Emr, S.D. (1998). Fab1p PtdIns(3)P 5-kinase function essential for protein sorting in the multivesicular body. Cell *95,* 847–858.

Raiborg, C., Bache, K.G., Mehlum, A., Stang, E., and Stenmark, H. (2001). Hrs recruits clathrin to early endosomes. EMBO J. *20,* 5008–5021.

Raiborg, C., Bache, K.G., Gillooly, D.J., Madshus, I.H., Stang, E., and Stenmark, H. (2002). Hrs sorts ubiquitinated proteins into clathrin-coated microdomains of early endosomes. Nat. Cell Biol. *4,* 394–398.

Rohn, W.M., Rouille, Y., Waguri, S., and Hoflack, B. (2000). Bi-directional trafficking between the trans-Golgi network and the endosomal/lysosomal system. J. Cell Sci. *113,* 2093–2101.

Rubino, M., Miaczynska, M., Lippe, R., and Zerial, M. (2000). Selective membrane recruitment of EEA1 suggests a role in directional transport of clathrin-coated vesicles to early endosomes. J. Biol. Chem. *275,* 3745–3748.

Sbrissa, D., Ikonomov, O.C., and Shisheva, A. (1999). PIKfyve, a mammalian ortholog of yeast Fab1p lipid kinase, synthesizes 5-phosphoinositides. Effect of insulin. J. Biol. Chem. *274,* 21589–21597.

Sbrissa, D., Ikonomov, O.C., and Shisheva, A. (2002a). Phosphatidylinositol 3-phosphate-interacting domains in PIKfyve. Binding specificity and role in PIKfyve. Endomenbrane localization. J. Biol. Chem. *277,* 6073–6079.

Sbrissa, D., Ikonomor. O.C., Deeb, A., and Shisheva, A. (2002b). Phosphatidylinositol 3,5-bisphosphate biosynthesis is linked to PIkfyve and is involved in osmotic response pathway in mammalian cells. J. Biol. Chem. *277,* 47276–47284.

Schu, P.V., Takegawa, K., Fry, M.J., Stack, J.H., Waterfield, M.D., and Emr, S.D. (1993). Phosphatidylinositol 3-kinase encoded by yeast VPS34 gene essential for protein sorting. Science *260,* 88–91.

Simonsen, A., Lippe, R., Christoforidis, S., Gaullier, J.M., Brech, A., Callaghan, J., Toh, B.H., Murphy, C., Zerial, M., and Stenmark, H. (1998). EEA1 links PI(3)K function to Rab5 regulation of endosome fusion. Nature *394,* 494–498.

Ullrich, O., Reinsch, S., Urbe, S., Zerial, M., and Parton, R.G. (1996). Rab11 regulates recycling through the pericentriolar recycling endosome. J. Cell Biol. *135,* 913–924.

Urbe, S., Mills, I.G., Stenmark, H., Kitamura, N., and Clague, M.J. (2000). Endosomal localization and receptor dynamics determine tyrosine phosphorylation of hepatocyte growth factor-regulated tyrosine kinase substrate. Mol. Cell. Biol. *20,* 7685–7692.

Wurmser, A.E., and Emr, S.D. (2002). Novel PtdIns(3)P-binding protein Etf1 functions as an effector of the Vps34 PtdIns 3-kinase in autophagy. J. Cell Biol. *158,* 761–772.